

✓  
UCRL- 84228  
PREPRINT

MASTER

CONF-800441--1

Field Reversal Produced by a Plasma Gun

Charles W. Hartman, W. Condit,  
E. Granneman, D. Prono, A.C. Smith, Jr.,  
J. Taska and W. C. Turner

This paper was prepared for submittal to  
International Symposium on Physics and  
Open-Ended Fusion Systems  
Tsukuba, Japan, April 15-18, 1980

April 2, 1980

 Lawrence  
Livermore  
Laboratory

This is a preprint of a paper intended for publication in a journal or proceedings. Since changes may be made before publication, this preprint is made available with the understanding that it will not be cited or reproduced without the permission of the author.

## Field Reversal Produced by a Plasma Gun\*

Charles W. Hartman, W. Condit, E.H.A. Granneman, \*\*  
D. Prono, A.C. Smith, Jr., \*\*\* J. Taska, W.C. Turner

Experimental results will be presented of the production of Field-Reversed Plasma with a high energy coaxial plasma gun. The gun is magnetized with solenoids inside the center electrode and outside the outer electrode so that plasma emerging from the gun entrains the radial fringe field at the muzzle. The plasma flow extends field lines propagating a field-reversed region along the external guide field. Ideally, because of high electrical conductivity, the flux inside the center electrode should be preserved. However, for low flux, the trapped flux exceeds by 2 or more the initial flux, possibly because of helical deformation of the current channel extending from the center electrode.

## I. Introduction

This paper reports in-progress studies of the production of reversed magnetic field, plasma-confinement configurations using a magnetized, coaxial plasma gun. The studies are directed toward forming and injecting the reversed-field configurations along an axial guide field in the  $\beta$  II apparatus<sup>1</sup> and then trapping the configuration in the magnetic mirror where energetic neutral beam heating will be applied to sustain the field-reversed mirror.

Application of coaxial guns to the production of field reversal was first investigated by Alfvén and coworkers.<sup>2</sup> Subsequent to these early studies at low energy it was recognized independently<sup>3</sup> that high energy, high efficiency, coaxial plasma guns currently developed could be applied to produce reversed-field plasma states approaching plasma conditions of interest for thermonuclear fusion studies. Further, if these and other studies indicate the coaxial gun approach is a viable means of start-up of a field-reversed mirror, extrapolation to reactor-scale systems appears

\* Work performed under the auspices of the U.S. Department of Energy by the Lawrence Livermore Laboratory under contract number W-7405-ENG-48.

\*\*On leave from FOM-Institute for Atomic and Molecular Physics, Amsterdam,  
The Netherlands.

\*\*\*PG&E Company, San Francisco, CA.

#### ANSWER

feasible.<sup>4</sup>

## II. Plasma Gun and Experimental Apparatus

The coaxial plasma gun used is shown schematically in Fig. 1. The design follows closely a high energy gun which has successfully produced Deuterium plasma with kinetic energy in the kilovolt region and total plasma energy of about 100 kJ.<sup>5</sup> The gun shown is driven by a  $C = 232 \mu F$ ,  $V \leq 40$  KV capacitor bank and has electrodes 1.5 m long with 0.15 m inner OD and 0.33 m outer ID. A significant difference in the present gun design is the introduction of pulsed solenoidal magnet windings shown in Fig. 1 which, when combined with the guide field, generate the field configuration shown in Fig. 2(a). An idealized model of field reversal is shown in Figs. 2(b) and 2(c). Here the field of Fig. 2(a), which is established before firing the gun, is extended by the plasma accelerated in the gun, Fig. 2(b), until field reconnection takes place to form an isolated, field-reversed plasma ring Fig. 2(c). Typically, the plasma conductivity is sufficiently high that nearly all the reversed magnetic flux within the inner electrode is trapped by the emerging plasma in this 2-dimensional model.<sup>6</sup> An important aspect of the above process is that the gun field  $B_\theta$  is imbedded in the plasma during acceleration and eventually forms a toroidal field in the isolated ring.

The experimental apparatus with plasma diagnostics is shown in Fig. 3. Only the gun-side of the vacuum tank and guide-field coils are shown. Further from the gun is a central mirror region with energetic neutral beam sources and a vacuum tank extension similar to that shown. A nearly uniform guide field of up to 6 kG is provided for 5 sec by the coils shown in Fig. 3. Diagnostics discussed in this paper consist of stainless-steel jacketed diamagnetic loops 60 cm in diameter, a jacketed  $B_r$  loop 60 cm in diameter, and jacketed magnetic probe arrays (.95 cm diameter) inserted into the plasma either as shown in Fig. 3 or from the end of the vacuum tank.

## III. Experimental Results

Before firing the gun, the guide field is established, the solenoidal windings are pulsed ( $\sim 5$  msec), and the pulse gas valve is opened releasing, typically, 50 Atm-cm<sup>3</sup>  $D_2$ . The gun is fired when the gas has expanded to roughly fill the interelectrode space. Since the current-sheath thickness and imbedded  $B_\theta$  field are dependent on the gas breakdown,<sup>7</sup> the performance

of the gun is critically dependent on the time delay of firing after gas injection.

After adjusting the gas delay to about one sound transit time from the gas valve to the breech for optimum performance, typical voltage, current, and energy input traces shown in Fig. 4 are obtained. Following bank-fire at  $t = 7 \mu\text{sec}$ , breakdown and acceleration occur and plasma emerges from the muzzle at  $17.5 \mu\text{sec}$ . Following voltage reversal ( $t = 19.0 \mu\text{sec}$ ) the insulator breaks down crowbarring the gun and at subsequent times the external voltage and current shown in Fig. 4 are determined by external circuit parameters while the current inside the gun (not directly measured) is determined by the dynamics of the current channel established in the accelerated plasma.

Figures 5(a) and (b) show measurements of the change in  $B_z$  (along  $B_{\text{guide}}$ ) on the gun axis for two probe positions,  $z = 80$  and  $130 \text{ cm}$  respectively. The azimuthally averaged radial field measured at  $z = 70 \text{ cm}$  is shown in Fig. 5(c), and diamagnetic loop signals at  $z = 63, 80, 131$ , and  $148.5 \text{ cm}$  are shown in Fig. 5(d) (The gun muzzle is located at  $z = 12.6 \text{ cm}$ ). From Fig. 5(a) it is seen that a strong field-reversal signal appears at  $t = 17.5 \mu\text{sec}$  and lasts roughly  $10 \mu\text{sec}$ . At  $z = 130 \text{ cm}$ , Fig. 5(b), the  $B_z$  signal appears about  $1 \mu\text{sec}$  later, and lasts about  $2 \mu\text{sec}$ . The  $B_r$  signal, Fig. 5c, shows first a negative spike corresponding to the field converging in the direction of plasma flow as the plasma emerges followed by a positive signal, indicating the field diverges in the direction of plasma flow, which decays and again goes negative. The diamagnetic loops show a propagating front with a velocity  $v_z \simeq 34 \text{ cm}/\mu\text{sec}$  and narrowing duration time as  $z$  increases.

An interpretation of Fig. 5 consistent with the data shown is that the accelerated plasma traps the poloidal flux in the center electrode and carries it away from the gun. Elongation of the field occurs (as in Fig. 2(b)) without reconnection until the plasma kinetic energy is given up to poloidal-field energy and then the stretched poloidal field accelerates the plasma back towards the gun.

The reversed flux  $\phi_t$  trapped by the plasma and carried to  $z = 80 \text{ cm}$  is shown in Fig. 6 versus the initial flux  $\phi_0$  in the center electrode.  $\phi_t$  was computed from simultaneous measurements of  $B_z$  along the  $y$  (vertical) axis using a 5-probe array. From Fig. 6 it is seen that the accelerated plasma efficiently entrains the initial flux. Amplification of  $\phi_0, \phi_t >$

$\phi_0$  is also seen to occur from Fig. 6 as was observed by the earlier Alfvén experiment.<sup>2</sup>

In general, the 5-probe array shows fluctuations which become more pronounced as  $\phi_0$  is decreased. Figure 7 shows y-axis profiles of  $\Delta B_z$  and  $B_x$  for  $\phi_0 = 918, 358$  and  $-23 \text{ kG-cm}^2$ . Fig. 7(a),  $\phi_0 = 918 \text{ kG-cm}^2$ , shows a relatively well centered reversed  $B_z$  profile at  $t = 10 \mu\text{sec}$ . At  $t = 25 \mu\text{sec}$  the y distribution has evolved to profiles which are not readily interpretable as a simple off-axis displacement. At  $\phi_0 = 358 \text{ kG-cm}^2$ , Fig. 7(b), by  $t = 21.25 \mu\text{sec}$  the field-reversed region has narrowed and appears displaced in the -y direction. Displacements, as shown, have been corroborated by 4 additional probes located in each quadrant of the x-y plane. Figure 7(c) shows an extreme case of small negative  $\phi_0$  (center-electrode flux in the same direction as  $B_{\text{guide}}$ ). Here large, rapid fluctuations occur and although reversed  $B_z$  is observed, no identifiable  $\Delta B_z, B_x$  profiles are seen.

#### IV. Summary and Conclusions

Limited magnetic probe data, which form the basis of this paper, indicate that for the conditions considered here, efficient entrainment of the initial vacuum poloidal flux occurs. Fluctuations occur during propagation of the field-reversed region away from the gun. The measured flux trapped usually exceeds the initial flux, particularly at low  $\phi_0$  and the fluctuations become more pronounced. These observations are consistent with the observations of Alfvén and coworkers<sup>2</sup> and consistent with the mechanism invoked as an explanation.<sup>2</sup>

A flux enhancement mechanism is illustrated in Fig. 8. Here the field-reversed region, in essence a stabilized z-pinch, extends from the gun center conductor as the result of the insulator breakdown crowbarring of the gun current. Helical kinking of the reversed-field region is expected to occur from MHD instabilities with the resulting helical current channel generating the enhancement poloidal field shown dashed. For fixed gun conditions, the crowbarred gun current ( 500 kA for the data here) would tend to be constant so that as  $\phi_0$  is reduced, tighter, more unstable pinches would occur consistent with the observed increase in fluctuations as  $\phi_0$  is decreased.

## References

1. W. C. Turner, et al., Nuc. Fusion 19, 1011 (1979).
2. H. Alfvén, et al., J. Nuc. Energy 1, 116 (1960).
3. C. W. Hartman, "A Use of Plasma Guns for Field-Reversed Mirrors," Tech. Memo, Jan. 12, 1978.
4. A. C. Smith, et al., "Startup of Field-Reversed Mirror Reactors Using Coaxial Guns," to be published as a Lawrence Livermore Laboratory report.
5. I. Hennins, J. Hammel, Bull. Am. Phys. Soc. 22, 1115 (1977).
6. J. Shearer, et al., Proc of the U.S.-Japan Joint Symposium on Compact Toruses and Energetic Particle Injection, 12-14 Dec. 1979, Princeton Plasma Physics Laboratory, p. 61.
7. J. Marshall, Proc. of the High Beta Workshop, Los Alamos Scientific Laboratory, July 28-Aug. 1, 1975, p. 470.

## NOTICE

This report was prepared as an account of work sponsored by the United States Government. Neither the United States nor the United States Department of Energy, nor any of their employees, nor any of their contractors, subcontractors, or their employees, makes any warranty, express or implied, or assumes any legal liability or responsibility for the accuracy, completeness or usefulness of any information, apparatus, product or process disclosed, or represents that its use would not infringe privately-owned rights.

Reference to a company or product name does not imply approval or recommendation of the product by the University of California or the U.S. Department of Energy to the exclusion of others that may be suitable.

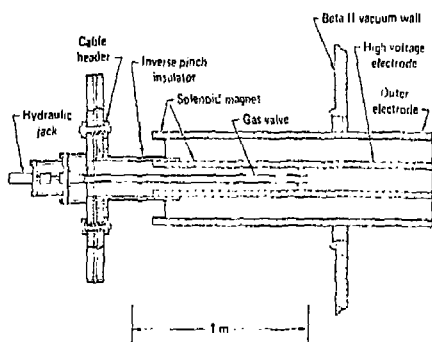


Fig. 1 Coaxial Plasma Gun

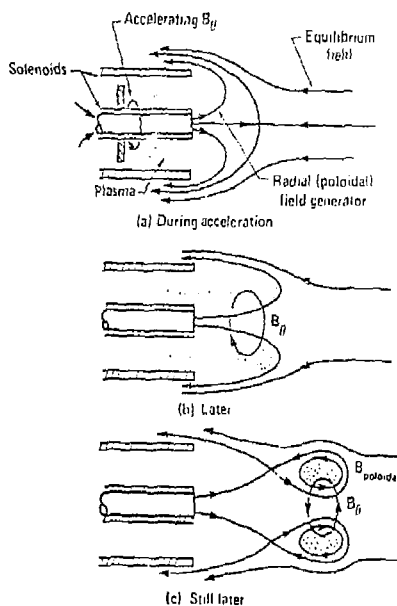
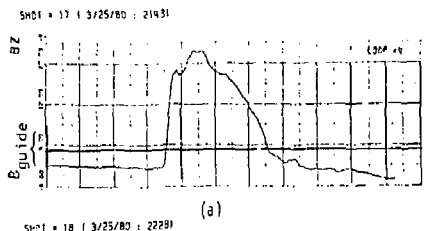
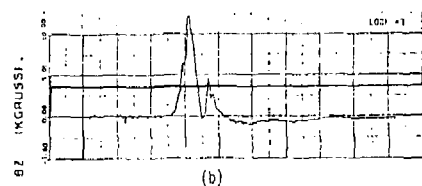


Fig. 2 Formation of Field-Reversed Plasma by a Coaxial Plasma Gun

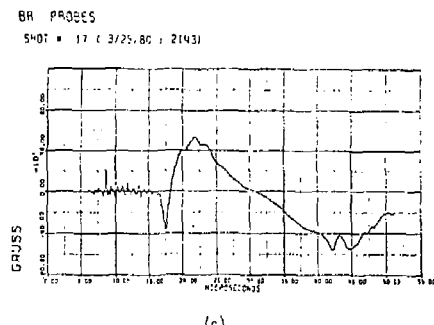




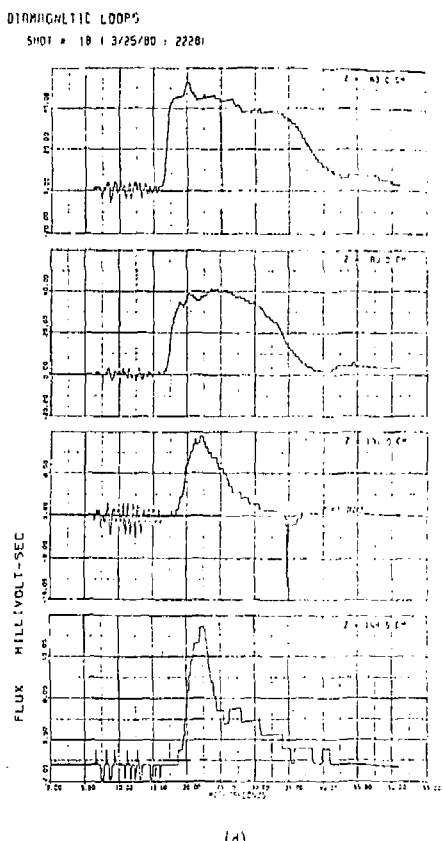
(a)



(b)



(c)



(d)

Fig. 5 (a) Change in  $B_z$  on axis at  $z = 80$  cm, the Guide field is  $B_{\text{guide}} = 3.1$  kG and upward directed signals represent diamagnetism and for,  $B_z > B_{\text{guide}}$ , field reversal. (b) Same as (a) at  $z = 130$  cm, (c)  $B_r$  at  $r = 30$  cm,  $z = 70$  cm, (d) Diamagnetic loop signals for the  $z$  positions indicated.

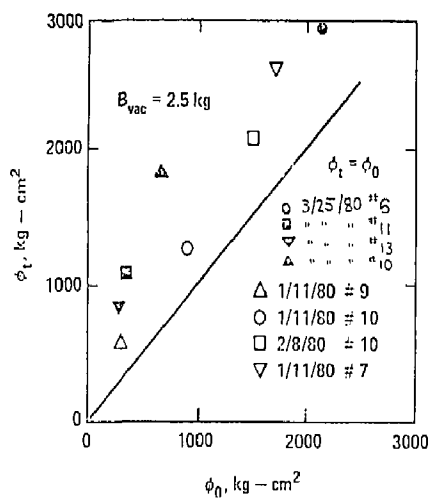


Fig. 6 Trapped flux  $\phi_t$  vs initial flux in the center electrode  $\phi_0$  at  $z = 80$  cm.

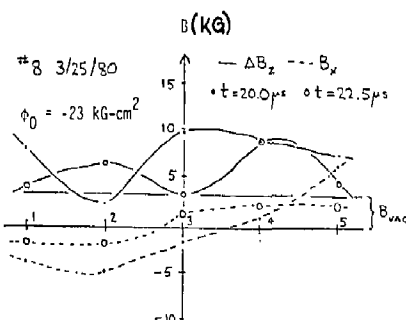
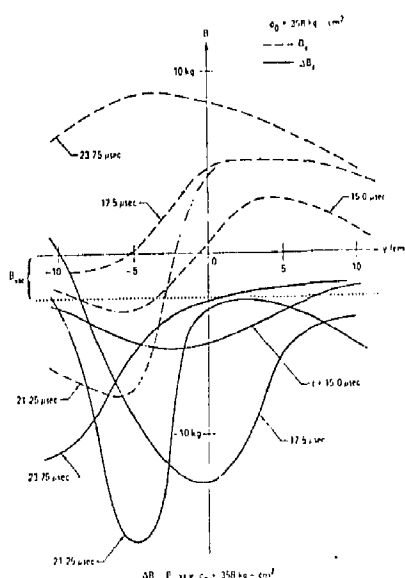
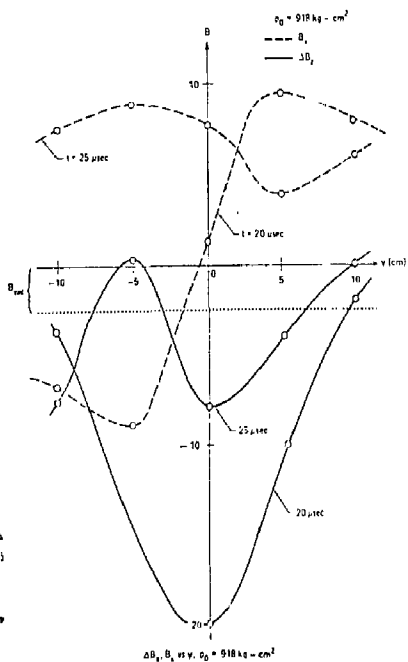


Fig. 7 (a)  $\Delta B_z$ ,  $B_x$  vs  $y$ ,  $\phi_0 = 918$  kg - cm\$^2, (b) same,  $\phi_0 = 358$  kg - cm\$^2, (c) same,  $\phi_0 = -23$  kg - cm\$^2.

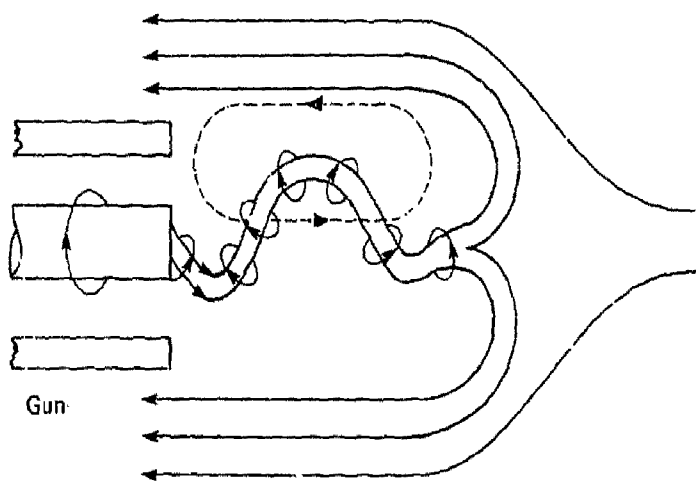


Fig. 8 Flux Enhancement by Kink Instability